Indian Journal of Production and Thermal Engineering (IJPTE)
ISSN: 2582-8029 (Online), Volume-5 Issue-5, August 2025

Effect of Channel Width on Flow Characteristics in PEM Fuel Cell Anode and Cathode Flow Fields – a CFD Study

J. Karthikeyan, Ragul Kumar Kittusamy

Abstract: ***The performance of Proton Exchange Membrane Fuel Cells (PEMFCs) is highly influenced by the geometric design of the flow field channels that deliver reactants and remove by-products. In this study, the effect of channel width in anode and cathode flow fields with a four-channel multiple-pass short serpentine (FCMPSS) configuration was investigated using Computational Fluid Dynamics (CFD) simulations in ANSYS Fluent under laminar flow conditions to identify optimal width combinations. The analysis includes three anode and cathode width combinations for a fixed channel depth of 1.25 mm and cell active area of 112 cm^2. The tested combinations are 0.8 mm, 1 mm, and 1.2 mm for the anode, and 0.6 mm, 0.8 mm, and 1 mm for the cathode, respectively. Flow rates are derived for the target current density of 0.7 A/cm^2. This study focuses on flow characteristics by excluding electrochemical reactions to understand the flow behaviour before incorporating electrochemical models, and was validated through a grid independence study and Reynolds number analysis. Simulation results showed that narrower channels significantly increase pressure drop and reactant velocity, thereby enhancing reactant convection and water removal. However, they can also increase reactant pumping power and the risk of membrane dehydration. Conversely, wider channels reduce pressure drop and velocity, thereby lowering pumping energy losses, but risk poor reactant distribution and local flooding. The configuration with 1.0 mm anode and 0.8 mm cathode widths achieved the most balanced performance, exhibiting moderate pressure drops of approximately 2044 Pa and 8822 Pa, and corresponding velocities of 4.76 m/s and 4.17 m/s, which support efficient transport phenomena while minimising energy losses.***

Keywords: PEM Fuel Cell, Channel Width, Flow Field Design, Numerical Study, Pressure Drop, Velocity Distribution.

Abbreviations:
PEMFC: Proton Exchange Membrane Fuel Cell
FCMPSS: Four-Channel Multi-Pass Short Serpentine
CFD: Computational Fluid Dynamics
GDL: Gas Diffusion Layer
MEA: Membrane Electrode Assembly
CAD: Computer-Aided Design
H_2: Hydrogen
O_2: Oxygen
AMG: Algebraic Multigrid
Re: Reynolds Number
2D: Two-Dimensional
ΔP: Change in Pressure
ΔV: Change in Velocity

Manuscript received on 11 June 2025 | First Revised Manuscript received on 21 June 2025 | Second Revised Manuscript received on 17 July 2025 | Manuscript Accepted on 15 August 2025 | Manuscript published on 30 August 2025.
*Correspondence Author(s)
Dr. J. Karthikeyan*, Fuel Cell Researcher, Chennai (Tamil Nadu), India. Email ID: jkshridi@gmail.com, ORCID ID: 0009-0000-8987-4553
Dr. Ragul Kumar Kittusamy, Chief Engineer Consultant - Fuel Cell Systems and Innovation, Rasa.AI Labs, Chennai (Tamil Nadu), India. Email ID: ragulkumar.kittusamy@rasaailabs.com, ORCID ID: 0000-0002-3459-3276

I. INTRODUCTION

Growing national concern over fossil fuel depletion and climate change has positioned the proton exchange membrane fuel cell (PEMFC) as a leading alternative power system for the automotive industry [1]. PEMFCs are attractive clean energy devices due to their low operating temperature, quick start-up, and high-power density [2]. Their performance and efficiency are critically influenced by the flow field design [3], which governs the transport of hydrogen and oxygen to reaction sites and the removal of water and heat.

In PEMFC stacks, the design of the anode and cathode flow fields is critical for uniform reactant distribution and efficient product removal. At higher power densities, increased water formation within the stack necessitates optimized flow field configurations to ensure effective water removal and prevent flooding [4]. Serpentine flow fields are commonly employed due to their ability to enhance convective mass transfer across the electrode surface [5]. However, single long serpentine channels can lead to significant pressure drops and reactant depletion along the flow path [6]. To mitigate these limitations, a four-channel multiple-pass short serpentine (FCMPSS) configuration was employed in this study, offering several advantages. Dividing the flow into multiple shorter channels connected in series or parallel reduces the overall pressure drop while maintaining a relatively long residence time for effective reactant utilization [7]. The multiple passes promote better cross-flow and under-rib convection within the gas diffusion layer (GDL), leading to a more uniform distribution of reactants and improved removal of product water, particularly in the cathode [8]. This enhanced mass transport uniformity ultimately contributes to higher overall fuel cell performance and durability compared to traditional single-pass serpentine designs.

Although PEMFC operation involves complex electrochemical reactions, preliminary flow field studies that exclude electrochemical reactions still offer valuable insights before proceeding with electrochemical flow analysis [9]. Accurate fluid flow and pressure distribution analysis helps identify optimal channel geometries, enabling designers to mitigate issues such as flooding, starvation, and excessive pressure drops before incorporating complete electrochemical modelling [10]. A moderate pressure drop across these

flow fields is essential to balance several competing factors such as sufficient reactant supply, mass transport, uniform distribution, and parasitic losses, which significantly influence fuel cell performance [11].

On the other hand, the reactant velocity in PEMFCs has a significant impact on their performance [12]. Low velocity leads to insufficient reactant delivery, increased concentration polarization, inadequate water removal (especially in the cathode), and non-uniform reactant distribution. Moderate velocity provides an optimal balance between reactant supply and product removal, efficient mass transport, relatively uniform distribution, and acceptable pressure drop. High velocity increases reactant delivery and improves water removal, but it results in a higher pressure drop, significant parasitic losses, and potential membrane dehydration [13]. Therefore, the flow field design must strike a balance: providing sufficient pressure drop with moderate velocity to ensure adequate reactant supply and mass transport, while minimising excessive pressure drop to avoid significant parasitic losses [14].

This study aims to design anode and cathode flow fields employing an FCMPSS flow configuration. Further, investigates the effect of varying channel width combinations on pressure drop and velocity distribution within the anode and cathode flow fields using CFD simulations.

II. FLOW FIELD DESIGN

The anode and cathode flow fields were designed in an FCMPSS configuration using SolidWorks. Each design incorporates four distributors that connect the manifold to the flow field at the inlet and vice versa at the outlet. The reactant entering the inlet manifold splits into four streams and then flows through the flow field. The flow field is situated within the active area of the PEM fuel cell, where the electrochemical reaction takes place via the membrane electrode assembly (MEA) positioned between the anode and cathode flow fields. Unconsumed reactants or reaction by-products are leaving the cell due to the pressure energy of the reactant flow. Table 1 presents the anode and flow field cases considered for CFD studies, and Figure 1 shows two-dimensional computer-aided design (2D-CAD) models of the following anode and cathode flow field combinations: a) A0.8 & C0.6, b) A1 & C0.8, and c) 1.2 & C1.

Table 1. Flow Field Cases Considered for CFD Studies

Flow field	Case	Channel Width (mm)	Channel Depth (mm)	No. of Passes per Channel	Total Length of Channels (mm)
Anode	A0.8	0.8	1.25	18	5471.16
	A1	1		15	4658.7
	A1.2	1.2		14	4412.46
Cathode	C0.6	0.6		20	5965.63
	C0.8	0.8		18	5471.16
	C1	1		15	4658.7

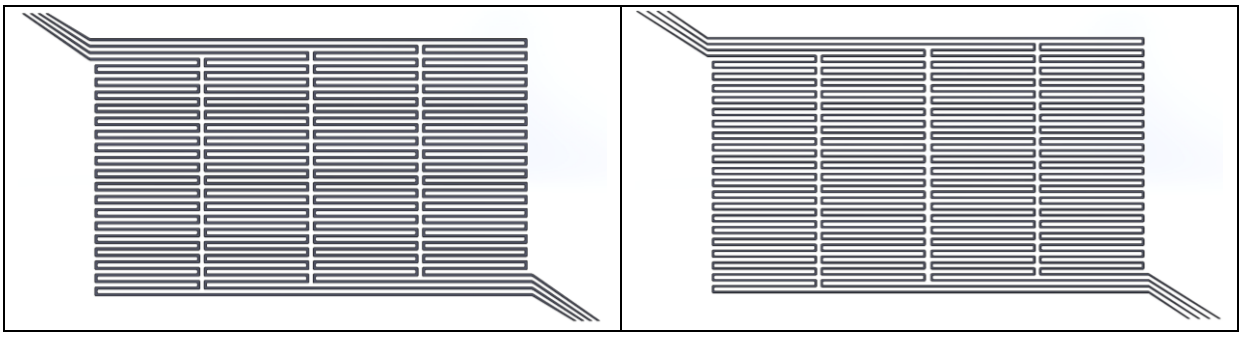

(a)

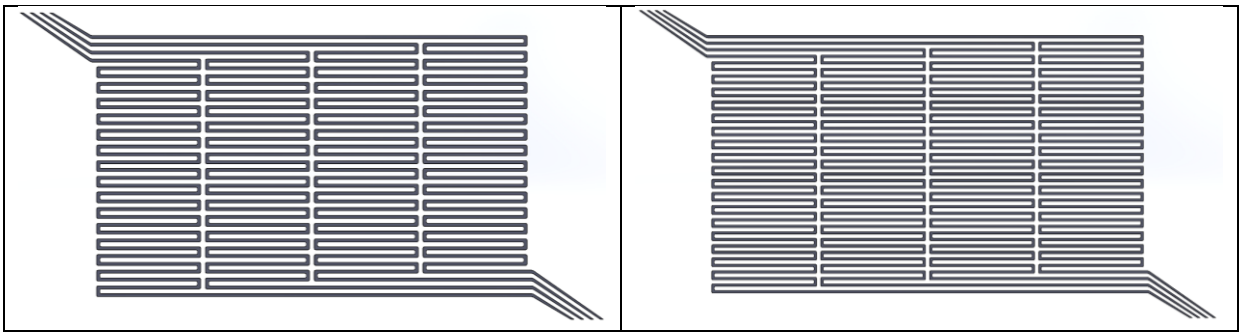

(b)

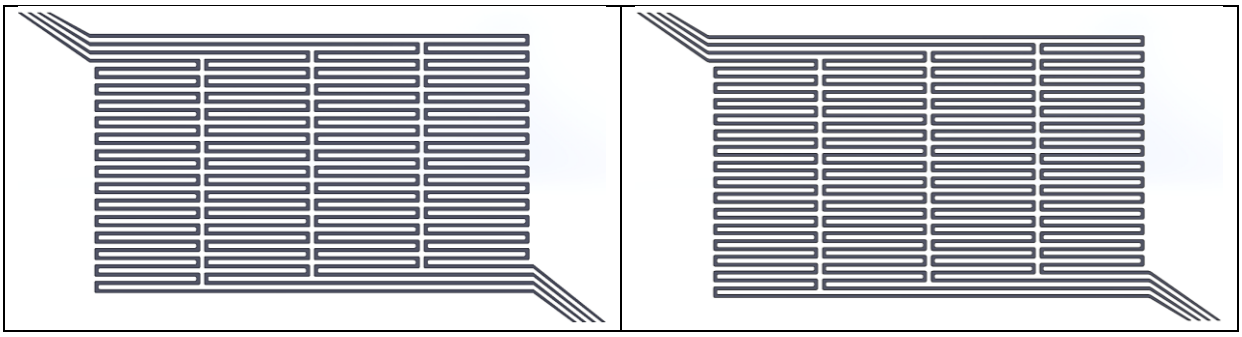

(c)

[Fig.1: 2D CAD Model of Anode and Cathode Flow Field Combinations a) A0.8 & C0.6, b) A1 & C0.8, and c) A1.2 & C1]

III. MATHEMATICAL MODELLING

A two-dimensional, steady-state simulation model, based on the incompressible Navier-Stokes equations with laminar flow assumptions, was employed [15]. The study did not include electrochemistry, heat transfer analysis, or the GDL. The incompressible Navier-Stokes equations are as follows:

Continuity equation:

$$\frac{\partial u}{\partial x} + \frac{\partial v}{\partial y} = 0 \quad \ldots \quad (1)$$

Momentum equation:

$$\rho\left(\frac{\partial u}{\partial t} + u\frac{\partial u}{\partial x} + v\frac{\partial u}{\partial y}\right) = -\frac{\partial p}{\partial x} + \mu\left(\frac{\partial^2 u}{\partial x^2} + \frac{\partial^2 u}{\partial y^2}\right) \quad \ldots \quad (2)$$

$$\rho\left(\frac{\partial v}{\partial t} + u\frac{\partial v}{\partial x} + v\frac{\partial v}{\partial y}\right) = -\frac{\partial p}{\partial y} + \mu\left(\frac{\partial^2 v}{\partial x^2} + \frac{\partial^2 v}{\partial y^2}\right) \quad \ldots \quad (3)$$

Where u and v are velocity vectors in the x and y direction, ρ and μ are the density and dynamic viscosity of the reactants. Commercial software, ANSYS Fluent R19.0, was employed to solve the governing equations. Boundary conditions were specified at the inlet and outlet for all models studied to solve the governing equations. Mass flow rates were fixed at the inlet, and the pressure was determined at the outlet. The boundary conditions imposed for computational modelling are as follows and illustrated in Figure 2.

Inlet boundary condition:

$$m_{inlet} = m_{in} \quad \ldots \quad (4)$$

Outlet boundary condition:

$$P_{outlet} = P_{out} \quad \ldots \quad (5)$$

Wall boundary condition:

A no-slip boundary condition was imposed for all walls and ribs.

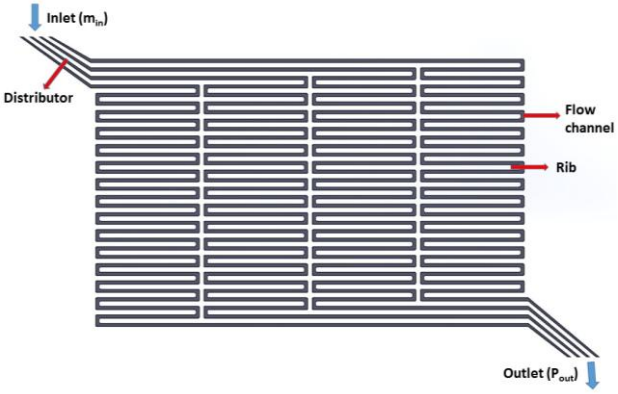

[Fig.2: FCMPSS's Fluid Domain and Boundary Conditions]

The working fluid used in this study was hydrogen (H2) for the anode and oxygen (O2) for the cathode flow fields. The initial mass flow rate for H_2 and O_2 was calculated using Equation (6) [16], as given below,

Mass flow rate of the reactants $m = \frac{N(\lambda iA)}{nf}$ (moles/sec) … (6)

N – Number of cells

λ – Stoichiometric ratio of reactants [17]

λ_{H_2} = 1.2 to 2

λ_{O_2} = 1.5 to 2

A – Active area of the cell (cm^2)

n – Number of electrons per molecule

n = 2 for H_2

n = 4 for O_2

f – Faraday's constant = 96,485 coulombs/electron-mole.

The obtained mass flow rate for H_2 is 9.755 x 10^{-7} kg/s, and O_2 is 1.3 x 10^{-5}. The outlet pressure for all cases was kept constant at atmospheric pressure, i.e., 0 bar gauge pressure. For the ANSYS simulations, the spatial discretization was handled with the following methods for the interpolation function. Gradients were calculated with the least

squares cell-based method. The pressure terms were discretized using a second-order scheme, and the momentum terms were discretized with a second-order upwind scheme. The algebraic multigrid (AMG) solver was used to solve the linear equation with under-relaxation factors of 0.3 for pressure and 0.7 for momentum. The convergence residual values for continuity and momentum (x, y, and z velocities) are maintained at 1 × 10^-6, respectively.

To ensure the numerical study had the proper number of elements and optimum computation time, a grid independence test was conducted. A quadrilateral linear mesh was generated for this study, and the change in pressure and velocity components was captured to determine the proper element size. Four different element sizes were used for this optimization study: 0.2 mm, 0.15 mm, 0.1 mm and 0.05 mm. Further decreasing the element size increases the total number of elements generated in a model, thereby reducing convergence difficulties. The numerical results for the grid independence test, using different element sizes and mesh parameters, are presented in Table 2.

Table 2. Grid Independence Study for A1 case

Element Size (mm)	No. of Elements	Skewness	Orthogonality	Element Quality	Inlet Pressure P_{in} (Pa)	Outlet Pressure P_{out} (Pa)	ΔP (Pa)	Inlet Velocity V_{in} (m/s)	Outlet Velocity V_{out} (m/s)	ΔV (m/s)
0.2	853370	3.23E-02	0.97966	0.977	460.8	28.8	432	5.819	0.3233	5.4957
0.15	1759976	5.97E-02	0.99435	0.9822	481.1	30.07	451.03	6.81	0.3783	6.4317
0.1	6118125	1.55E-02	0.99711	0.99385	544.9	34.01	510.89	7.62	0.3233	7.2967
0.05	11712450	1.22E-02	0.99876	0.99921	546.2	33.72	512.48	7.77	0.3022	7.4678

The grid independence study shows that ΔP and ΔV are very close for element sizes of 0.1 and 0.05. Thus, considering accuracy and iteration time, an element size of 0.1 mm was chosen. This element size was used for all models in this paper because the active areas, rib and channel sizes for all models were the same. The velocity and pressure distributions of the four flow field designs were compared using simulation models.

IV. THEORETICAL VALIDATION OF LAMINAR FLOW ASSUMPTION

For the flow to be laminar in a rectangular duct, the Reynolds (Re) number should be < 2300 [18]. The Re can be calculated as follows,

From the continuity equation,

Volumetric flow rate of the reactant is $Q = A_c v$ (m^3/sec) … (7)

A_c – Cross-sectional area of the channel (m^2)

v – Velocity of the reactant (m/s)

Reynolds number, $Re = \frac{\rho D_h v}{\mu}$ … (8)

ρ – Density of the reactant (kg/m^3)

D_h – Hydraulic diameter $= \frac{2\,(d \times w)}{d + w}$

d – Depth of the channel (m)

w – Width of the channel (m)

v – Velocity of the reactants (m/s)

μ – Dynamic viscosity of the reactants (kg-m/s)

$\mu_{H_2} = 0.84 \times 10^{-5}$ kg-m/s

$\mu_{O_2} = 2.064 \times 10^{-5}$ kg-m/s

Using Equations (7) and (8), the Reynolds numbers for all the considered study cases were calculated, and the results are presented in Table 3. For all the instances, the calculated Re values were consistently below the critical threshold of 2300, thereby confirming that the flow regime was laminar. Consequently, the assumption of laminar flow is validated for the present CFD studies.

Table 3. Reynolds Numbers for the Study Cases

Anode width (mm)	Reynolds number (Re)	Cathode width (mm)	Reynolds number (Re)
0.8	328.82	0.6	2184.60
1	281.84	0.8	1764.48
1.2	250.53	1	1512.41

V. RESULTS AND DISCUSSION

A. Pressure Drop Analysis

The pressure distribution within the anode and cathode flow fields for each channel width combination is illustrated in Figure 3. The pressure drop results are summarized in Table 4.

Anode **Cathode**

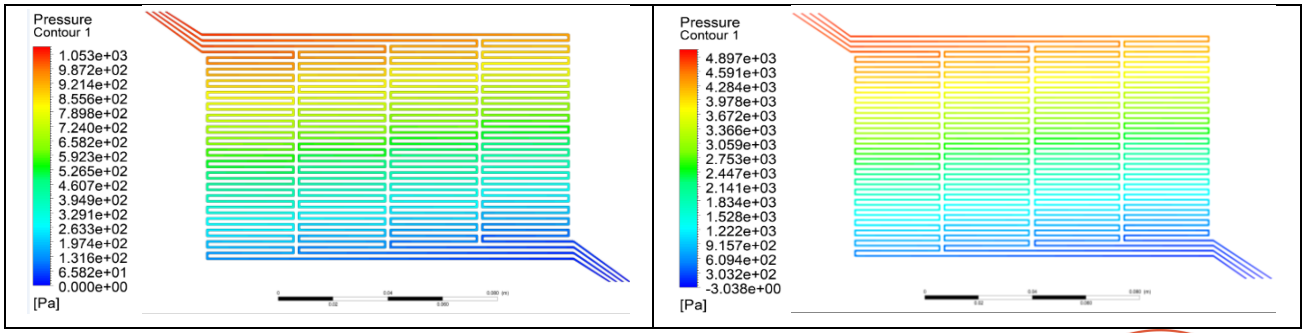

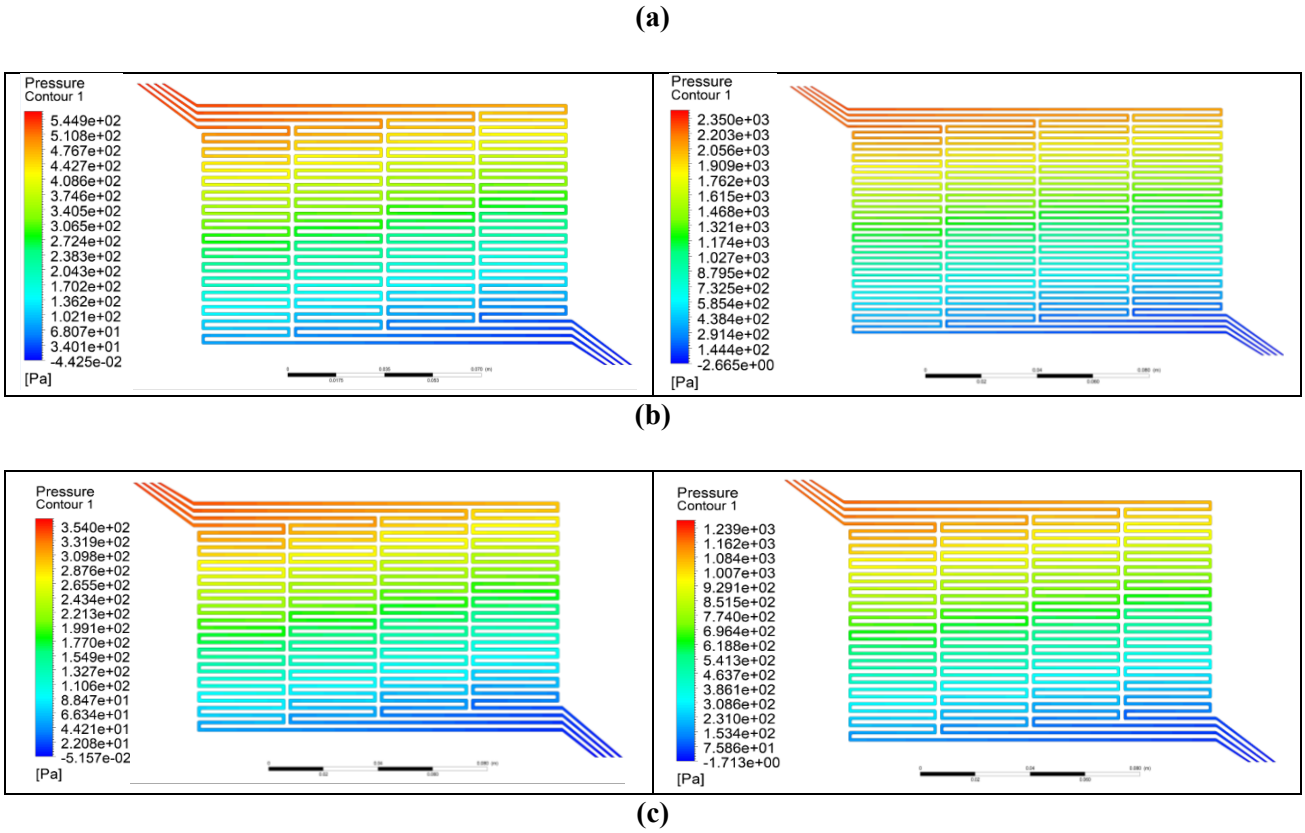

[Fig.3. Pressure Contours of Anode and Cathode Flow Field Combinations: a) A0.8 & C0.6, b) A1 & C0.8, and c) 1.2 & C1]

On the anode side, it was observed that as the channel width increased from 0.8 mm to 1.2 mm, the total pressure drop decreased significantly. Specifically, the narrowest channel (A0.8) exhibited a total pressure drop of 3948.72 Pa (0.040 bar), whereas the widest channel (A1.2) exhibited the lowest total pressure drop of 1328 Pa (0.013 bar). This trend can be attributed to the larger cross-sectional area of the flow, which reduces flow resistance.

Similarly, on the cathode side, a decrease in pressure drop was observed as the channel width increased. The narrowest cathode channel (C0.6) showed a substantially higher total pressure drop of 18,375.2 Pa (0.180 bar) compared to the C1 case, which demonstrated a pressure drop of 4652.56 Pa (0.047 bar).

Table 4. Total Pressure Drop in the Anode and Cathode Flow Field Channels

Anode width (mm)	Pressure Drop per Channel (Pa)	Total Pressure Drop (Pa)	Total Pressure Drop (bar)	Cathode width (mm)	Pressure Drop per Channel (Pa)	Total Pressure Drop (Pa)	Total Pressure Drop (bar)
0.8	987.18	3948.72	0.040	0.6	4593.8	18375.2	0.180
1	511	2044	0.020	0.8	2205.6	8822.4	0.088
1.2	332	1328	0.013	1	1163.14	4652.56	0.047

This inverse relationship between channel width and pressure drop is attributed to the reduced hydraulic resistance in wider channels, facilitating more effortless reactant flow. However, excessive widening can compromise reactant distribution and water management, especially on the cathode side. The higher pressure drop in narrower channels enhances reactant transport but leads to increased parasitic losses, which is undesirable for overall fuel cell efficiency [19].

Among all combinations, the A1 and C0.8 configuration achieved a balanced performance
with moderate pressure drops (2044 Pa for the A1 case and 8822.4 Pa for the C0.8 case), ensuring effective reactant transport while limiting parasitic energy losses incurred for pumping reactants into the stack.

B. Velocity distribution

The velocity contours for different channel width combinations are shown in Figure 4. Additionally, the average velocities within the flow fields were calculated and summarized in Table 5.

As expected, narrower channels led to higher average velocities due to the smaller flow cross-sectional area for the same mass flow rate. In the anode flow field, the average velocity decreased from 5.81 m/s (for A0.8 case) to 3.75 m/s (for A1.2 case) as the channel width increased. Similarly, in the cathode flow field, the average velocity decreased from 5.12 m/s (for the C0.6 case) to 3.40 m/s (for the C1 case).

Higher average velocities in narrow channels enhance reactant convection and promote efficient water removal, which is especially critical for cathode operation. However, they also contribute to greater pressure drops and can risk membrane dehydration if excessively high. Conversely, lower velocities in wider channels favour reduced parasitic losses but may risk insufficient reactant delivery and water

accumulation, potentially leading to local flooding and performance degradation [20].

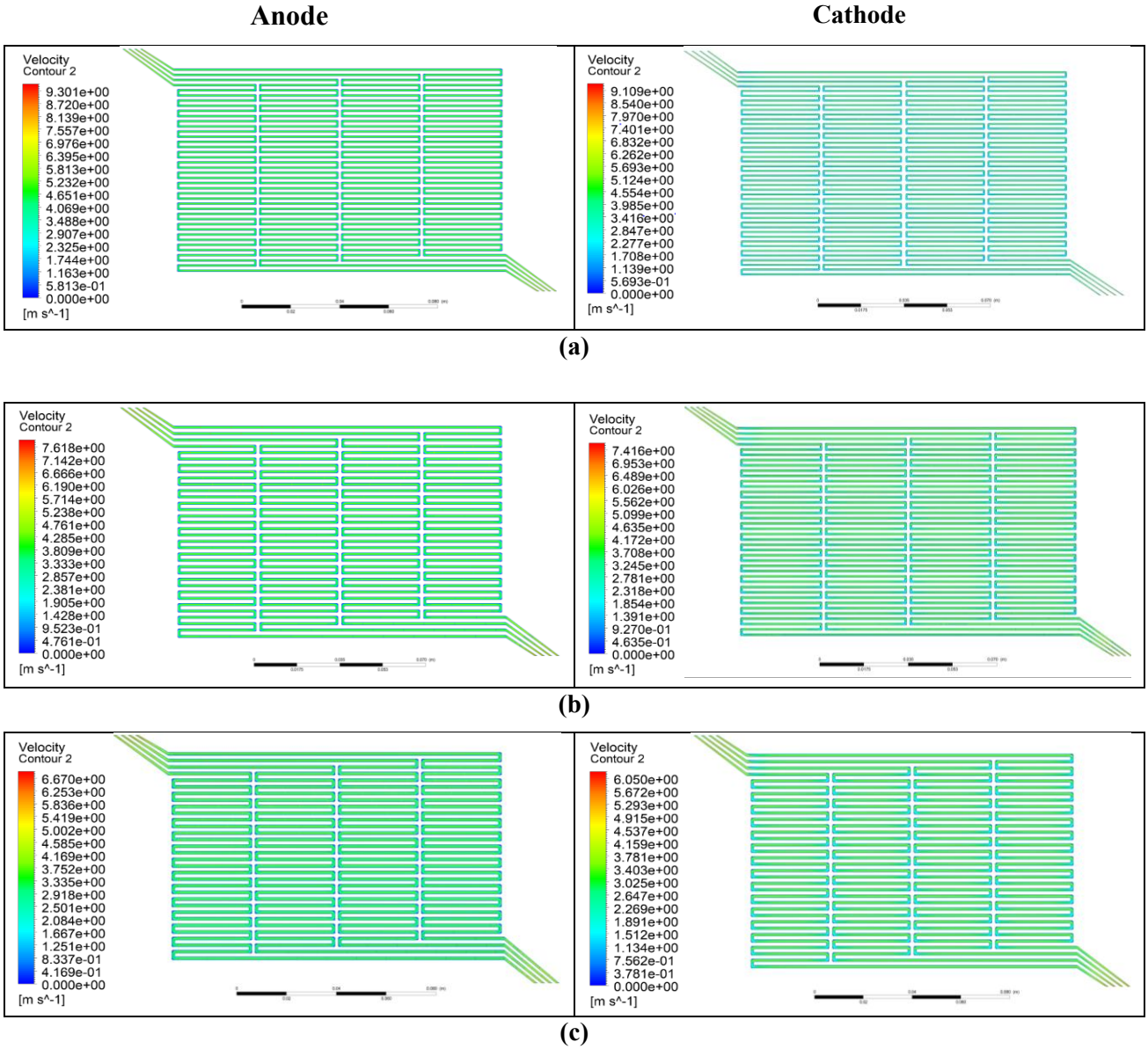

[Fig.4: Velocity Contours of Anode and Cathode Flow Field Combinations: a) A0.8 & C0.6, b) A1 & C0.8, and c) 1.2 & C1]

Table 5. Average Velocities for Different Anode and Cathode Channel Widths

Anode width (mm)	Average velocity (m/s)	Cathode width (mm)	Average velocity (m/s)
0.8	5.81	0.6	5.12
1.0	4.76	0.8	4.17
1.2	3.75	1.0	3.40

Among the studied cases, the A1 and C0.8 configuration, with an anode average velocity of 4.76 m/s and a cathode average velocity of 4.17 m/s, provided an optimal moderate velocity range. This balance supports uniform reactant distribution and efficient water management without introducing significant energy penalties or membrane drying risks, making it the most promising combination.

VI. CONCLUSION

This CFD study investigated the influence of channel width variations on the flow characteristics within the anode and cathode flow fields of a PEMFC employing a 4CMPSS configuration under laminar conditions, providing a foundational understanding of flow behaviour before incorporating electrochemical models. The results showed a clear inverse relationship between channel width and both pressure drop and flow velocity. Narrower channels resulted in higher pressure drops and average velocities, enhancing reactant convection, which can increase the reactant pumping power and the risk of membrane dehydration. Conversely, wider channels reduce pressure drops and velocities, which can minimise reactant pumping power but potentially compromise reactant delivery and water removal efficiency.

Among the studied cases, the 1 The 0.8 mm anode (A0.8) and 0.8 mm cathode (C0.8) widths provided the most balanced

Retrieval Number: 100.1/ijpte.E202905050825
DOI: 10.54105/ijpte.E2029.05050825
Journal Website: www.ijpte.latticescipub.com

Published By:
Lattice Science Publication (LSP)

performance. This case maintained moderate pressure drops (2044 Pa at the anode and 8822 Pa at the cathode) and average velocities (4.76 m/s at the anode and 4.17 m/s at the cathode), ensuring efficient reactant distribution, effective water management, and minimised parasitic losses. These results underscore the crucial importance of optimising channel dimensions to strike a delicate balance between fluid dynamic resistance, reactant transport, and overall fuel cell performance. These findings provide a valuable reference point for further research involving electrochemical reactions, multi-physics coupling, and comprehensive performance evaluation for practical PEMFC applications.

DECLARATION STATEMENT

After aggregating input from all authors, I must verify the accuracy of the following information as the article's author.

- **Conflicts of Interest/ Competing Interests:** Based on my understanding, this article has no conflicts of interest.
- **Funding Support:** This article has not been funded by any organizations or agencies. This independence ensures that the research is conducted with objectivity and without any external influence.
- **Ethical Approval and Consent to Participate:** The content of this article does not necessitate ethical approval or consent to participate with supporting documentation.
- **Data Access Statement and Material Availability:** The adequate resources of this article are publicly accessible.
- **Author's Contributions:** The authorship of this article is contributed equally to all participating individuals.

REFERENCES

1. Md Shehan Habib, Paroma Arefin, Md Abdus Salam, Kawsar Ahmed, Md Sahab Uddin, Tareq Hossain, Nasrin Papri and Tauhidul Islam (2025), Proton Exchange Membrane Fuel Cell (PEMFC) Durability Factors, Challenges, and Future Perspectives: A Detailed Review, Material Science Research India, vol. 18 (2), 217-234. DOI: http://dx.doi.org/10.13005/msri/180209
2. Yuan Qin, Houcheng Zhang, Xinfeng Zhang (2022), Integrating high-temperature proton exchange membrane fuel cell with duplex thermoelectric cooler for electricity and cooling cogeneration, International Journal of Hydrogen Energy, vol. 47 (91), 38703-38720. DOI: https://doi.org/10.1016/j.ijhydene.2022.09.041
3. Sadiq T. Bunyan, Hayder A. Dhahad, Dhamyaa S. Khudhur, Talal Yusaf (2023), Effect of a Novel Flow Field Design on PEM Fuel Cell Performance, 16th International Conference on Developments in eSystems Engineering (DeSE), IEEE, 156-161. DOI: https://doi.org/10.1109/DeSE60595.2023.10469060
4. Rohit Gupta, Mohit Gupta, Brijendra Kumar Sharma (2022), Study of PEM Fuel Cell for Different Cell Temperatures, Indian Journal of Advanced Physics (IJAP), vol. 2 (1), 26-30. DOI: https://doi.org/10.54105/ijap.A1038.042122
5. Fang-Bor Weng, Mangaliso Menzi Dlamini, Jenn-Jiang Hwang, (2023), Evaluation of flow field design effects on proton exchange membrane fuel cell performance, International Journal of Hydrogen Energy, vol. 48 (39), 14866-14884. DOI: https://doi.org/10.1016/j.ijhydene.2023.01.005
6. Fırat Isikli, Hazal Isikli & Ali Surmen, (2025), Effect of Number of Channels on Performance of PEM Fuel Cells for Serpentine Type Channel Configuration, Arabian Journal for Science and Engineering, vol. 50, 2595–2612. DOI: https://doi.org/10.1007/s13369-024-09199-9
7. Firat Isikli · Hazal Isikli, Ali Surmen, (2025), Effect of Number of Channels on Performance of PEM Fuel Cells for Serpentine Type Channel Configuration, Arabian Journal for Science and Engineering, vol. 50, 2595–2612. DOI: https://doi.org/10.1007/s13369-024-09199-9
8. Sadiq T. Bunyan, Hayder A. Dhahad, Dhamyaa S. Khudhur, and Talal Yusaf, (2023), The Effect of Flow Field Design Parameters on the Performance of PEMFC: A Review, MDPI: Sustainability, vol. 15 (13), 10389; DOI: https://doi.org/10.3390/su151310389
9. Hossein Pourrahmani, Adel Yavarinasab, Majid Siavashi, Mardit Matian, Jan Van herle, (2022), Progress in the proton exchange membrane fuel cells (PEMFCs) water/thermal management: From theory to the current challenges and real-time fault diagnosis methods, Energy Reviews, vol. 1 (1), 100002, DOI: https://doi.org/10.1016/j.enrev.2022.100002
10. B.H. Lim, E.H. Majlan, W.R.W. Daud, M.I. Rosli, T. Husaini, (2017), Numerical analysis of modified parallel flow field designs for fuel cells, International Journal of Hydrogen Energy, vol. 42 (14), 9210-9218, DOI: https://doi.org/10.1016/j.ijhydene.2016.03.189
11. M. Rahimi-Esbo, A.A. Ranjbar, A. Ramiar, E. Alizadeh, M. Aghaee, (2016), Improving PEM fuel cell performance and effective water removal by using a novel gas flow field, International Journal of Hydrogen Energy, vol. 41 (4), 3023-3037, DOI: https://doi.org/10.1016/j.ijhydene.2015.11.001
12. Wenjie Qi, Xin Chen, Zhi Gang Zhang, Shuaishuai Ge, Huan Wang, Ruxin Deng, Zilin Liu, Jiying Tuo, ShengChang Guo, Junjie Cheng (2024), Performance of the multi-U-style structure-based flow field for polymer electrolyte membrane fuel cell, Scientific Reports, vol. 14, 23318. DOI: https://doi.org/10.1038/s41598-024-74257-z
13. Gurbinder Kaur, (2021), PEM Fuel Cells: Fundamentals, Advanced Technologies, and Practical Application, Elsevier book, DOI: https://doi.org/10.1016/C2020-0-00143-X
14. Hao Chen, Hang Guo, Fang Ye, Chong Fang Ma, (2020), An experimental study of cell performance and pressure drop of proton exchange membrane fuel cells with baffled flow channels, Journal of Power Sources, vol. 472, 228456, DOI: https://doi.org/10.1016/j.jpowsour.2020.228456
15. Andrei Kulikovsky, (2023), Laminar Flow in a PEM Fuel Cell Cathode Channel, Journal of The Electrochemical Society, vol. 170, 024510, DOI: https://doi.org/10.1149/1945-7111/acba47
16. Mehmet Fatih Orhan, Kenan Saka, and Mohammad Yousuf, (2022), Design and Optimization of Fuel Cells: A Case Study on Polymer Electrolyte Membrane Fuel Cell Power Systems for Portable Applications, Hindawi: Advances in Polymer Technology, ID 6568456, vol. 10, DOI: https://doi.org/10.1155/2022/6568456
17. S. Chevalier1, J C. Olivier, C. Josset, and B. Auvity (2019), Polymer electrolyte membrane fuel cell operating in stoichiometric regime, Journal of Power Sources, vol. 440, 227100, DOI: https://doi.org/10.1016/j.jpowsour.2019.227100
18. Odysseas Gkionis-Konstantatos, Luciana Tavares, Thomas Ebel (2024), Investigating the Role of Flow Plate Surface Roughness in Polymer Electrolyte Membrane Fuel Cells with the Use of Multiphysics Simulations, MDPI: Batteries, vol. 10 (8), 276, DOI: https://doi.org/10.3390/batteries10080276
19. Suprava Chakraborty, Devaraj Elangovan, Karthikeyan Palaniswamy, Ashley Fly, Dineshkumar Ravi, Denis Ashok Sathia Seelan, Thundil Karuppa Raj Rajagopal, A Review on the Numerical Studies on the Performance of Proton Exchange Membrane Fuel Cell (PEMFC) Flow Channel Designs for Automotive Applications, MDPI: Energies, vol. 15 (24), 9520. DOI: https://doi.org/10.3390/en15249520
20. Rashed Kaiser, Chi-Yeong Ahn, So-Yeon Lee, Yun-Ho Kim, Jong-Chun Park, (2025), Numerical Analysis of Water Management and Reactant Distribution in PEM Fuel Cells with a Convergent 5-Channel Serpentine Flow Field for Emission-Free Ships, International Journal of Naval Architecture and Ocean Engineering, 100649. DOI: https://doi.org/10.1016/j.ijnaoe.2025.100649

AUTHOR'S PROFILE

Dr. Karthikeyan Janakiraman holds a Ph.D. in Artificial Intelligence and Hydrogen Fuel Cells, with over 23 years of industry experience spanning AI/ML, Generative AI, and sustainable energy systems. He leads innovation at the intersection of artificial intelligence, clean energy, and enterprise transformation. His work drives impactful change across the BFSI, energy, and manufacturing sectors, combining strategic vision with deep technical expertise. His core research areas include AI-enabled performance modelling and optimization of proton exchange membrane fuel cells (PEMFCs), intelligent risk detection systems, and sustainable technology architectures. With multiple patents granted in both AI and clean energy, Dr. Karthikeyan is recognized for driving high-impact innovation across emerging technologies and complex system landscapes. He has successfully led AI integration efforts across control systems, operational intelligence, and predictive analytics, while also playing an active role in mentoring tech talent. His contributions span academia, consultancy, and corporate leadership—emphasizing practical deployment of intelligent systems in

high-regulation domains. A strong advocate of inclusive growth and knowledge-sharing, Dr. Karthikeyan remains committed to research, education, and community-driven development. He continues to support advanced R&D in AI and clean energy technologies through strategic collaborations and thought leadership.

Dr. Ragul Kumar Kittusamy holds a Ph.D. in Mechanical Engineering under the prestigious AICTE National Doctoral Fellowship program by MHRD – Government of India, with a strong focus on sustainable energy systems. His core research areas include phase change material-based thermal energy storage (TES) and proton exchange membrane fuel cells (PEMFC), with demonstrated expertise in both CFD analysis and experimental validation. He has worked extensively on the thermal management of PEMFC stacks, including BoP subsystems and cooling strategies. He is currently involved in an AI-integration project with control systems for real-time fuel cell monitoring and control. His academic and industrial experiences span consultancy, teaching, and product development, with a focus on innovation in low-carbon technologies. With publications in reputed international journals and an Indian patent, he continues to support advanced R&D in clean energy technologies as a consultant in fuel cell systems.